

University of Wollongong Research Online

Faculty of Engineering - Papers (Archive)

Faculty of Engineering and Information Sciences

2012

Angular-dependences of giant in-plane and interlayer magnetoresistances in Bi 2Te 3 bulk single crystals

Z J. Yue
University of Wollongong, zy709@uowmail.edu.au

Xiaolin Wang University of Wollongong, xiaolin@uow.edu.au

S X. Dou University of Wollongong, shi@uow.edu.au

http://ro.uow.edu.au/engpapers/5110

Publication Details

Yue, Z. J., Wang, X. L. & Dou, S. X. (2012). Angular-dependences of giant in-plane and interlayer magnetoresistances in Bi 2Te 3 bulk single crystals. Applied Physics Letters, 101 (15), 152107-1-152107-4.

 $Research\ Online\ is\ the\ open\ access\ institutional\ repository\ for\ the\ University\ of\ Wollongong.\ For\ further\ information\ contact\ the\ UOW\ Library:\ research-pubs@uow.edu.au$



Angular-dependences of giant in-plane and interlayer magnetoresistances in Bi2Te3 bulk single crystals

Z. J. Yue, X. L. Wang, and S. X. Dou

Citation: Appl. Phys. Lett. 101, 152107 (2012); doi: 10.1063/1.4756941

View online: http://dx.doi.org/10.1063/1.4756941

View Table of Contents: http://apl.aip.org/resource/1/APPLAB/v101/i15

Published by the American Institute of Physics.

Related Articles

Magnetic and magnetotransport properties of Ba2FeMoO6 pulsed laser deposited thin films J. Appl. Phys. 112, 083923 (2012)

Ultra-high hole mobility exceeding one million in a strained germanium quantum well Appl. Phys. Lett. 101, 172108 (2012)

On the estimation of the magnetocaloric effect by means of microwave technique AIP Advances 2, 042120 (2012)

Parallel-leaky capacitance equivalent circuit model for MgO magnetic tunnel junctions Appl. Phys. Lett. 101, 162404 (2012)

Influence of Fe segregation at grain boundaries on the magnetoresistance of Sr2Fe1+δMoO6 polycrystals J. Appl. Phys. 112, 073925 (2012)

Additional information on Appl. Phys. Lett.

Journal Homepage: http://apl.aip.org/

Journal Information: http://apl.aip.org/about/about the journal Top downloads: http://apl.aip.org/features/most_downloaded

Information for Authors: http://apl.aip.org/authors

ADVERTISEMENT

Universal charged-particle detector for interdisciplinary applications:

- Non-scanning Mass Spectrometry
- Non-scanning Ion Mobility Spectrometry Non-scanning Electron Spectroscopy
- Direct microchannel plate readout
- Thermal ion motion and mobility studies
 Bio-molecular ion soft-landing profiling
- Real-time beam current/shape tuning
- Diagnostics tool for instrument design Compact linear array for beam lines

Contact OI Analytical: +1-205-733-6900



Angular-dependences of giant in-plane and interlayer magnetoresistances in Bi₂Te₃ bulk single crystals

Z. J. Yue, X. L. Wang, ^{a)} and S. X. Dou Spintronic and Electronic Materials Group, Institute for Superconducting and Electronic Materials, University of Wollongong, NSW 2522, Australia

(Received 8 July 2012; accepted 18 September 2012; published online 11 October 2012)

Angular-dependences of in-plane and interlayer magnetotransport properties in *n*-type Bi₂Te₃ bulk single crystals have been investigated over a broad range of temperatures and magnetic fields. Giant in-plane magnetoresistances (MR) of up to 500% and interlayer MR of up to 200% were observed, respectively. The observed MR exhibits quadratic field dependences in low fields and linear field dependences in high fields. The angular dependences of the MR represent strong anisotropy and twofold oscillations. The observed angle-dependent, giant MR might result from the strong coulomb scattering of electrons as well as impurity scattering in the bulk conduction bands of *n*-type Bi₂Te₃. The strong anisotropy of the MR may be attributable to the anisotropy of electron mobility, effective mass, and relaxation time in the Fermi surface. The observed giant anisotropic MR in *n*-type Bi₂Te₃ bulk single crystals paves the way for Bi₂Te₃ single crystals to be useful for practical applications in magnetoelectronic devices such as disk reading heads, anisotropic magnetic sensors, and other multifunctional electromagnetic applications. © *2012 American Institute of Physics*. [http://dx.doi.org/10.1063/1.4756941]

Bismuth telluride (Bi₂Te₃) has a rhombohedral structure, space group R_{3m} (D^{5}_{3d}), and is well-known as a narrow gap (band gap energy, $E_{\rm g} \approx 0.2\,{\rm eV}$) layered semiconductor. In the past few years, Bi₂Te₃ crystals have been intensively studied because of their excellent thermoelectric performance at the vicinity of room temperature. 2,3 And, Bi₂Te₃ based semiconductors have been widely applied in thermoelectric energy converters, refrigerators, and thermostats operating near room temperatures. Recently, Bi₂Te₃ compounds were confirmed as three-dimensional topological insulators by angle resolved photoemission spectroscopy (ARPES) measurements and band structure calculations. Topological insulators have been mainly investigated by ARPES, scanning tunneling microscopy (STM), and theoretical calculations. 6 Topological insulators are quantum materials with insulating bulk states and topologically protected metallic surface states. They have fascinating electronic properties and potential applications in quantum information processing, magnetoelectric devices, and other spintronics.

The electrical properties and band structure parameters of Bi_2Te_3 have been systemically studied through magneto-transport measurements within the last few decades. The Hall effect, Shubnikov-de Haas effect (SdH), and the thermoelectric effect have been investigated in Sb, Sn, Ag, and Ga doped Bi_2Te_3 . A many-valley model was applied to estimate several parameters, including the shape and orientation of the energy ellipsoids, as well as the density of carriers and the relaxation time. The transverse MR effect (defined as $(R_B - R_0/R_0) \times 100\%$ with R_B and R_0 the resistance with and without magnetic field, respectively) has also been studied in a Bi_2Te_3 crystal annealed at 410 °C. The observed MR value at 1.8 K is 200% with a field of 9 T applied along

the c-axis. The anisotropy of the electrical conductivity in *n*-type Bi₂Te₃ has been measured and the mass parameters of the ellipsoids were calculated with the six-valley ellipsoid model in the isotropic relaxation time approximation. 13-15 Recently, Aharonov-Bohm oscillations have also been observed in Bi₂Se₃ and Bi_{1-x}Sb_x topological insulators. ^{16,17} Non-saturating positive linear MR (LMR) of up to 22% and 50% at high fields and low temperature was observed in Bi₂Se₃ films and nanoribbons. ^{18,19} Very recently, we have observed room temperature giant and linear MR in the topological insulator Bi₂Te₃ in the form of nanosheets.²⁰ The thickness of Bi₂Te₃ nanosheets is only 20 nm, corresponding to about 20 QL layers and the applied magnetic field is perpendicular to the direction of current. The giant, linear MR achieved is as high as over 600% at room temperature without any sign of saturation at measured fields up to 13 T. The observed linear MR was attributed to the quantum linear MR model developed by Abrikosov.²¹ The observed LMR could possibly allow topological insulators to be implemented as magnetic sensors regardless of its source.

Angular-dependent in-plane MR and Shubnikov-de Haas oscillations have been studied in topological insulators Bi₂Se₃, Bi_{1-x}Sb_x, PbS single crystals.²²⁻²⁴ The observed angular-dependent oscillations can be well simulated by using the parameters obtained from the Shubnikov-de Haas oscillations, which clarify that the oscillations are essentially due to the bulk Fermi surface. The results pave the way to distinguish the 2D surface states from 3D bulk states in angular-dependent MR studies by completely elucidating the bulk oscillations. Motivated by these experiments, here, we investigated the angular-dependences of in-plane and interlayer MR in *n*-type Bi₂Te₃ bulk single crystals. Angular-dependent MR does not display Shubnikov-de Haas oscillations, however, giant, high field linear, in-plane MR of up to 500%, and interlayer MR of up to 200% were observed in Bi₂Te₃ bulk single crystals.

^{a)}Author to whom correspondence should be addressed. Electronic mail: xiaolin@uow.edu.au.

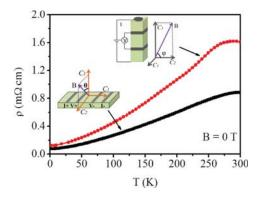


FIG. 1. In-plane and interlayer resistivity of n-type Bi_2Te_3 as a function of temperatures in B=0 T. The insets show schematic diagrams for the measurements of in-plane (black squares) and interlayer (red circles) MR.

Both in-plane and interlayer MR display strong angular-dependences and twofold oscillations, especially at low temperatures and high magnetic fields. Our experimental results show that the $\mathrm{Bi}_2\mathrm{Te}_3$ bulk single crystals also have potential applications in anisotropic magnetoelectronic devices such as anisotropic magnetic sensors.

The n-type Bi₂Te₃ single crystals used for this study were cleaved from the same bulk crystals (with 99.99% purity) that were used in Ref. 20. In the procedures for the inplane magnetotransport measurements, four-probe transport measurements were performed on a rectangular sample between T = 2 K and T = 300 K using a Quantum Design 14T Physical Properties Measurement System (PPMS). The size of the sample was $4 \times 3 \times 0.16$ mm³, and the distance d between the two inner contacts was 1 mm. The resistances were obtained by applying an electric current I (500 μ A) through the two outer silver contacts and monitoring the voltage drop V between the two inner contacts, as shown in Fig. 1. The current I was applied in the plane and the magnetic field B was applied in the C_2C_3 plane, perpendicular to the current direction. For some selected magnetic field directions, the field dependences of the in-plane MR were measured by sweeping B between 0 and 13 T. Rotation of the sample in constant magnetic field B was used to measure the MR. In the procedures for the interlayer magnetotransport measurements, four-probe transport measurements were also performed on a rectangular sample between 2K and 300K using the same PPMS. The size of the sample was $3.28 \times 1.15 \times 1.15 \text{ mm}^3$, and the distance between the two inner contacts was 1 mm. The current for the interlayer magnetotransport measurements was $5000 \,\mu\text{A}$ and was applied along the C_3 axis while the magnetic field B was applied in C_2C_3 plane.

The temperature dependences of the in-plane and interlayer resistivity of *n*-type Bi₂Te₃ bulk single crystals were measured in B = 0 T. As shown in Fig. 1, the in-plane and interlayer resistivities decrease with the temperature and do not stay constant until T = 10 K. Compared with the in-plane resistivity, the interlayer resistivity is about twice as large. Such metallic R (T) curves are typical bulk behavior for ntype Bi₂Te₃ and result from the electron-type bulk carriers induced by Bi-Te antisite defects. At high temperatures, the scattering is predominantly governed by phonons and defects scattering, while at low temperatures the dominant scattering is electron Coulomb scattering in the valleys of conduction bands. The topological surface states are masked by the bulk states because of the high carrier concentration, so that the magnetotransport studied here mainly results from bulk transport properties. Figure 2(a) shows the in-plane MR measured at several degrees, ranging from $\theta = 0^{\circ}$ to $\theta = 180^{\circ}$, in B = 13 T at T = 2 K. The maximum value of the in-plane MR reaches up to 500% in B = 13 T at θ = 180°. Linear and non-saturating MR is clearly observed in high fields at $\theta = 135^{\circ}$ and $\theta = 180^{\circ}$ in positive B, but the linear MR is greatly suppressed at $\theta = 0^{\circ}$, $\theta = 45^{\circ}$, and $\theta = 90^{\circ}$ in positive B. The dependence of MR linearity on the angles of magnetic fields might result from the anisotropic Coulomb scattering of carriers with open orbits or close orbits due to the anisotropy of valleys. Figure 2(b) shows the interlayer MR versus magnetic field from B = 0 to B = 13 T, measured at different degrees. The maximum interlayer MR reaches up to 200% in B = 13 T at $\theta = 0^{\circ}$. At low magnetic fields, the interlayer MR exhibits quadratic field dependences, which can be fitted by $MR = kB^2$, with k a constant. The patterns of interlayer MR curves evolve linearly in high magnetic fields over all selected degrees. It is evident that the high field linear MR arises from the anisotropic bulk transport of the Bi₂Te₃ bulk with its layered crystal structures.

Figure 3(a) displays the angular-dependences of the inplane MR in n-type ${\rm Bi}_2{\rm Te}_3$ measured at B = 13 T for various temperatures. The temperature T, ranging from 2 to 300 K, was kept constant during each rotation. The observed angular-dependences of the MR display strong anisotropy and twofold oscillations. The MR values increase with decreasing temperature over all angles. The peaks appear at around $\theta = 0^\circ$ and $\theta = 180^\circ$, while the dips are at around $\theta = 90^\circ$ and $\theta = 270^\circ$. This suggests that the in-plane MR is much larger in interlayer high fields. Figure 3(b) shows the angular-dependences of the in-plane MR measured in different magnetic fields at 2 K. The magnetic field B, ranging from 1 to 13 T, was kept constant during each rotation. The

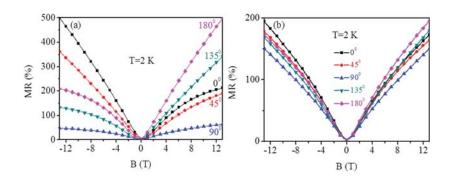


FIG. 2. (a) In-plane MR in n-type Bi_2Te_3 as a function of magnetic fields at several temperatures. (b) Interlayer MR in n-type Bi_2Te_3 as a function of magnetic fields at several angles.

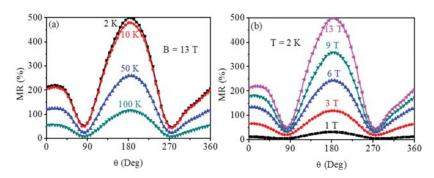


FIG. 3. (a) Angular-dependences of in-plane MR in n-type Bi_2Te_3 at B=13 T at different temperatures. (b) Angular-dependences of in-plane MR in n-type Bi_2Te_3 at T=2 K in different magnetic fields.

observed angular-dependences of the MR also display twofold oscillations, and the MR values increase with increasing magnetic fields. Figure 4(a) shows the angular-dependences of the interlayer MR measured in different temperatures T, ranging from T = 2 K to T = 300 K, in B = 13 T. Figure 4(b) displays the angular-dependences of the interlayer MR measured at different magnetic fields B, ranging from B = 1to B = 13 T, at T = 2 K. The observed angular-dependences of the interlayer MR also display strong anisotropy and twofold oscillations. Wide peaks in the interlayer MR curves appear at around $\theta = 0^{\circ}$ and 180° , and dips at around $\theta = 90^{\circ}$ and 270°. This suggests that the interlayer MR is most strongly pronounced when magnetic fields are perpendicular to the current direction. The MR anisotropic oscillations are also most strongly pronounced in high fields and low temperatures.

The well established Kohler's rule suggests that the MR of a material is a universal function of B as a result of the Lorentz force deflection of carriers, and at high fields, MR will saturate in most materials. Therefore, such a giant, anisotropic, non-saturating MR as in our n-type Bi₂Te₃ bulk crystals is unusual. Linear quantum-MR theory was originally developed by Abrikosov, based on gapless semiconductors and semiconductors at the extreme quantum limit to explain the observed giant linear MR in doped silver chalcogenides.²⁵ As stated above, in our previous work, the observed linear MR was attributed to the quantum linear MR from the surface states of topological insulators.²⁰ Metals that contain Fermi surfaces with open orbital in some crystallographic directions, including Cu, Ag, and Au, will also exhibit large linear MR for fields applied in those directions.²⁶ LMR can also occur in semiconductors as a consequence of strong electrical disorder, which is related to the carrier mobility, but is independent of carrier density.²⁷ The well known anisotropic MR is always observed in ferromagnetic materials, which results from s-d scattering. ²⁸ In addition, anisotropic MR also can result from the anisotropy of the Fermi surface because of the anisotropic effective mass and scattering effects. ²⁹

The giant, high-field linear, in-plane, and interlayer MR, with twofold anisotropic oscillations, in our samples is likely to be related to the configurations of the bulk conduction bands. The Fermi surfaces in n-type Bi₂Te₃ are approximately ellipsoids with rotational symmetry around the C_3 axis, with a small amount of trigonal warping. The Fermi surface consists of six ellipsoids tilted at an angle to the basal plane, where the two conduction bands are responsible for conduction. 10 The conduction bands are multivalley bands and consist of upper and lower conduction bands. Both conduction bands are filled by electrons with different mobility, effective mass, and relaxation time in different valleys.8 The non-saturating linear MR suggests that electrons have open orbits along the Fermi surface, because the MR should saturate at high B if the orbits are closed in high fields.²³ The main mechanisms of scattering in n-type Bi₂Te₃ are acoustic phonon scattering, impurity scattering, and coulomb scattering in conduction bands. The giant MR might come from electron coulomb scattering in the lower conduction band and from impurity scattering from doping induced impurity bands. 23 Furthermore, the upper and lower conduction bands in Bi₂Te₃ are anisotropic, due to the anisotropy of the ellipsoidal electron pockets with different mobility and relaxation time, which results in the observed giant anisotropic in-plane and interlayer MR. 11,12

In conclusion, we measured angular-dependent in-plane and interlayer MR of n-type $\mathrm{Bi_2Te_3}$ bulk single crystals in different magnetic fields, temperatures, and angles. Giant, high field linear, in-plane MR of up to 500%, and interlayer MR of up to 200% were observed. Both in-plane and interlayer MR represent strong anisotropy and twofold oscillations. The giant anisotropic MR might result from strong in-plane and interlayer electron coulomb scattering with anisotropic mobility and relaxation time in bulk conduction bands. Our results show that n-type $\mathrm{Bi_2Te_3}$ bulk single

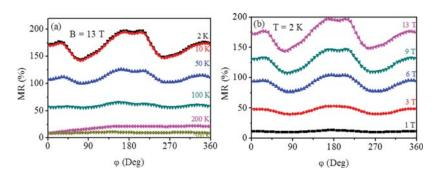


FIG. 4. (a) Angular-dependences of interlayer MR in n-type Bi₂Te₃ at B = 13 T at different temperatures. (b) Angular-dependences of interlayer MR in n-type Bi₂Te₃ at T = 2 K in different magnetic fields.

crystals have potential applications in anisotropic magnetic sensors and other multifunctional electromagnetic devices.

This work is partially supported by funding from the Australian Research Council under a Discovery Project (DP1094073).

- ¹V. A. Kulbachinski, H. Ozaki, Y. Miyahara, and K. Funagai, J. Exp. Theor. Phys. 97, 1212 (2003).
- ²C. B. Satterthwaete and R. W. Ure, Jr., Phys. Rev. **108**, 1164 (1957).
- ³H. Y. Lv, H. J. Liu, L. Pan, Y. W. Wen, X. J. Tan, J. Shi, and X. F. Tang, Appl. Phys. Lett. **96**, 142101 (2010).
- ⁴D. Kong, Y. L. Chen, J. J. Cha, Q. F. Zhang, J. G. Analytis, K. J. Lai, Z. K. Liu, S. S. Hong, K. J. Koski, S. K. Mo, Z. Hussain, I. R. Fisher, Z. X. Shen, and Y. Cui, Nat. Nanotechnol. 6, 705 (2011).
- ⁵J. S. Zhang, C. Z. Chang, Z. C. Zhang, J. Wen, X. Feng, K. Li, M. H. Liu, K. He, L. L. Wang, X. Chen, Q. K. Xue, X. C. Ma, and Y. Y. Wang, Nat. Commun. 2, 574 (2011).
- ⁶X. L. Qi and S. C. Zhang, Rev. Mod. Phys. **83**, 1057 (2011).
- ⁷M. Z. Hasan and C. L. Kane, Rev. Mod. Phys. **82**, 3045 (2010).
- ⁸V. A. Kulbachinskii, M. Inoue, M. Sasaki, H. Negishi, W. X. Gao, K. Takase, Y. Giman, P. Lostak, and J. Horak, Phys. Rev. B **50**, 16921 (1994).
- ⁹V. A. Kulbachinskii, A. Yu Kaminsky, R. A. Lunin, K. Kindo, Y. Narumi, K. Suga, S. Kawasaki, M. Sasaki, N. Miyajima, P. Lostak, and P. Hajek, Semicond. Sci. Technol. 17, 1133 (2002).
- ¹⁰R. B. Mallinson, J. A. Rayne, and R. W. Ure, Jr., Phys. Rev. 175, 1049 (1968).
- ¹¹H. A. Ashworth and J. A. Bayne, Phys. Rev. B **3**, 2646 (1971).

- ¹²Y. S. Hor, D. Qu, N. Pong, and R. J. Cava, J. Phys.: Condens. Matter 22, 375801 (2010).
- ¹³R. T. Delves, A. E. Bowley, D. W. Hazelden, and H. J. Goldsmid, Proc. Phys. Soc. **78**, 838 (1961).
- ¹⁴L. P. Caywood, Jr. and G. R. Miller, Phys. Rev. B **2**, 3209 (1970).
- ¹⁵H. A. Ashworth and J. A. Rayne, Phys. Lett. A **30**, 231 (1969).
- ¹⁶H. L. Peng, K. J. Lai, D. S. Kong, S. Meister, Y. L. Chen, X. Qi, S. C. Zhang, Z. X. Shen, and Y. Cui, Nature Mater. 9, 225 (2010).
- ¹⁷A. A. Taskin and Y. Ando, Phys. Rev. B **80**, 085303 (2009).
- ¹⁸H. T. He, B. K. Li, H. C. Liu, X. Guo, Z. Y. Wang, M. H. Xie, and J. N. Wang, Appl. Phys. Lett. **100**, 032105 (2012).
- ¹⁹H. Tang, D. Liang, R. L. J. Qiu, and X. P. A. Gao, ACS Nano 5, 7510 (2011).
- ²⁰X. L. Wang, Y. Du, S. X. Dou, and C. Zhang, Phys. Rev. Lett. 108, 266806 (2012).
- ²¹A. A. Abrikosov, Phys. Rev. B **58**, 2788 (1998).
- ²²K. Eto, Z. Ren, A. A. Taskin, K. Segawa, and Y. Ando, Phys. Rev. B 81, 195309 (2010).
- ²³A. A. Taskin, K. Segawa, and Y. Ando, Phys. Rev. B 82, 121302(R) (2010).
- ²⁴K. Eto, A. A. Taskin, K. Segawa, and Y. Ando, Phys. Rev. B 81, 161202(R) (2010).
- ²⁵A. A. Abrikosov, Phys. Rev. B **60**, 4231 (1999).
- ²⁶D. Stroud and F. P. Pan, Phys. Rev. B **20**, 455 (1979).
- ²⁷H. G. Johnson, S. P. Bennett, R. Barua, L. H. Lewis, and D. Heiman, Phys. Rev. B 82, 085202 (2010).
- ²⁸P. Wiśniewski, Appl. Phys. Lett. **90**, 192106 (2007).
- ²⁹Z. W. Zhu, A. Collaudin, B. Fauqué, W. Kang, and K. Behnia, Nat. Phys. 8, 89 (2012).